

**PREPARATION AND CHARACTERIZATION OF CROSS LINKED  
CHITOSAN FILLED CHITOSAN COMPOSITES**

**by**

**NURHIDAYATULLAILI MUHD JULKAPLI**

**Thesis submitted in fulfillment of the requirements**

**for the degree of**

**Doctor of Philosophy**

**June 2012**

## **ACKNOWLEDGEMENT**

If chitosan proud with its strong and durable glycosidic linkage, so do I. I am really proud of my research team. To both of my supervisor Prof. Dr. Hazizan Md Akil and Prof. Madya Dr. Zulkifli Ahmad, thanks for the strong and durable linkage that have made us still remain in one team despite all the challenges and obstacles. Thanks for being internally and externally resist and patience throughout the years of this research works.

If chitosan proud with its reactive and accessible functional groups, I am also proud to be a part of reactive and always accessible research places. To dean (Prof. Dr. Ahmad Fauzi b. Mohd Noor) and staff of School of Materials and Mineral Resources Engineering (USM), School of Industrial Technology (USM) and Advances Materials Research Centre (SIRIM) a lots of thanks for your assistance, kindness, knowledge, chances, trust, guidance, criticism, encouragement and opinions that really inspired me to complete this research works.

If chitosan proud with its renewable and sustainable sources, so do I which I am really proud with my research financial sources. To Ministry of Science Technology and Innovative (Malaysia) thank you for the scholarship (National Science Fellowship) and research grant (Fundamental Research Grant Scheme: 6070027). The special gratitude is also delivered to Institute of Postgraduate Studies (USM) for an extra budget under RU Post Graduate Research Grant (RUPGRG) and Graduate Assistance Scheme (GAS).

If chitosan proud with its supported C6 glucose ring, so do I which I am really proud with my research supporters. To my parents (Muhd Julkapli Isab and Sazanah Selamat), family members and friends for being around anywhere and at anytime I need. I owe a great many thanks for their time, idea, money, care, love, moral support and attention. Most importantly, my very most special thanks are dedicated to the One above all of us, the Almighty ALLAH, for answering my prayers and for giving me the strength to plod on despite my constitution wanting to give up and throw in the towel.

Like chitosan and its variety of contributions, hopefully, the little effort made in this research work will give some significant contribution on the development of bio-polymer knowledge's.

## TABLE OF CONTENTS

	Pages
<b>Acknowledgments</b>	ii
<b>Table of Contents</b>	iv
<b>List of Tables</b>	X
<b>List of Figures</b>	xi
<b>List of Symbols</b>	xv
<b>List of Abbreviation</b>	xviii
<b>Abstrak</b>	xx
<b>Abstract</b>	xxii
<b>CHAPTER 1- INTRODUCTION</b>	1
1.0 Overview	1
1.1 Cs bio-composites	1
1.2 Problem statements	6
1.3 Hypothesis of Cs/XCs bio-composites	9
1.4 Objectives of research	10
<b>CHAPTER 2-LITERATURE REVIEW</b>	11
2.0 Cs bio-composites	
<b>CHAPTER 3- MATERIALS AND METHODOLOGY</b>	12
3.0 Overview	12
3.1 Materials	12
3.1.1 Cs powders	12
3.1.2 Acid anhydride (AA) based cross linking agents	12
3.1.3 Organic solvent	13
3.1.4 Solid chemicals	14
3.1.5 pH buffer solutions	14
3.2 Methodology	15
3.2.1 Purification of raw materials	15

3.2.1.1 Purification of Cs powder	15
3.2.1.2 Distillation of NMP solvent	17
3.2.2 Preparation of XCs filler	19
3.2.2.1 Synthesis of XCs filler	19
3.2.2.2 Purification of XCs filler	20
3.2.3 Preparation of Cs/XCs bio-composites	21
3.2.4 Characterization of Cs, XCs and Cs/XCs bio-composites	
3.2.4.1 Chemical properties	22
3.2.4.1a Fourier Transform Infra-red (FTIR) analysis	22
3.2.4.1b <sup>1</sup> H and <sup>12</sup> C Nuclear Magnetic Resonance ( <sup>1</sup> H <sup>12</sup> C NMR) analysis	23
3.2.4.1c Elemental analysis	24
3.2.4.1d Energy Dispersive X-ray Spectroscopy (EDXS) analysis	24
3.2.4.2 Physical properties	24
3.2.4.2a X-ray diffraction (XRD) analysis	24
3.2.4.2b Particle size analysis	25
3.2.4.2c Density analysis	26
3.2.4.2d Viscosity analysis	26
3.2.4.2e Thickness analysis	27
3.2.4.3 Thermal properties	27
3.2.4.3a Thermogravimetry (TG) analysis	27
3.2.4.3b Differential Scanning Calorimetry (DSC) analysis	28
3.2.4.3c Dynamic Mechanical (DM) analysis	29
3.2.4.4 Morphology properties	29
3.2.4.4a Fields Emission Scanning Electron Microscope (FESEM) analysis	29
3.2.4.4b Acid digestion analysis	30

3.2.4.5 Solubility properties	30
3.2.4.6 Swelling properties	31
3.2.4.6a Swelling analysis of Cs and XCs	31
3.2.4.6b Swelling analysis of Cs/XCs bio-composites	31
3.2.4.7 Mechanical properties	32
3.2.4.7a Tensile analysis	32
3.2.4.7b Tearing analysis	33
<b>CHAPTER 4- PREPARATION AND CHARACTERIZATION OF XCs FILLER</b>	<b>34</b>
4.0 Overview	34
4.1 Published data	34
4.1.1 Preparation and characterization of BTC	34
4.1.2 Degree of crystallinity of XCs samples	35
4.2 Un-published data	36
4.2.1 Synthesis of XCs samples	36
4.2.1.1 Mechanism of cross linking	36
4.2.1.2 Total yield	39
4.2.2 Characterization of XCs filler	40
4.2.2.1 Chemical properties	40
4.2.2.1a Fourier Transform Infra-Red (FTIR) analysis	40
4.2.2.1b Solid state Nuclear Magnetic Resonance (NMR) analysis	46
4.2.2.1bi Solid state H Nuclear Magnetic Resonance ( $^1\text{H}$ NMR) analysis	46
4.2.2.1bii Solid state C Nuclear Magnetic Resonance ( $^{12}\text{C}$ HMR) analysis	49

4.2.2.1c	Energy Dispersive X-ray Spectroscopy (EDXS) analysis	53
4.2.2.1d	Elemental analysis	56
4.2.2.2	Physical properties	58
4.2.2.2a	Bulk density analysis	58
4.2.2.2b	Particle size analysis	60
4.2.2.2c	Field Emission Scanning Electron Microscopy (FESEM) analysis	62
4.2.2.3	Solubility properties	65
4.2.2.4	Swelling properties	67
4.2.2.5	Thermal properties	70
4.2.2.5a	Thermogravimetry (TG) analysis	70
4.2.2.5b	Differential Scanning Calorimetry (DSC) analysis	75
<b>CHAPTER 5- PREPARATION AND PROPERTIES OF Cs/XCs BIO-COMPOSITES</b>		82
5.0	Overview	82
5.1	Published data	82
5.1.1	Preparation and properties of Cs/BTC bio-composites	82
5.1.2	Preparation and properties of Cs/ODAC bio-composites	84
5.1.3	Preparation and properties of Cs/DPAC bio-composites	84
5.2	Un-published data	85
5.2.1	Preparation of bio-composites mixture	85
5.2.1.1	Viscosity	86
5.2.2	Physical properties	89
5.2.2.1	Thickness	90
5.2.3	Interfacial bonds	92
5.2.3.1	Fourier Transform Infra-Red (FTIR)	92

analysis	
5.2.4 Dispersion	92
5.2.5 Mechanical properties	95
5.2.5.1. Tensile properties	95
5.2.5.2 Tearing properties	102
5.2.5.3 An optimization on mechanical properties	109
5.2.5.4 Morphology analysis of fracture surfaces	111
5.2.5.4a Fracture surface analysis under tensile mode	111
5.2.5.4b Fracture surface analysis under tearing mode	116
5.2.6 Thermal properties	121
5.2.6.1 Thermogravimetry (TG) analysis	121
5.2.6.2 Differential Scanning Calorimetry (DSC) analysis	127
5.2.6.3 Dynamic Mechanical (DM) analysis	133
5.2.6.4 An optimization on thermal properties	136
5.2.7 Hydrophilicity properties	142
5.2.7.1 Acidic medium	143
5.2.7.2 Neutral medium	150
5.2.7.3 Alkaline medium	155
5.2.7.4 An optimization on hydrophilic properties	160
<b>CHAPTER 6- LIST OF PUBLISHED DATA</b>	163
6.1 Paper I	163
6.2 Paper II	164
6.3 Paper III	165
6.4 Paper IV	166
6.5 Paper V	167
6.6 Paper VI	168
6.7 Paper VII	169



<b>CHAPTER 7- CONCLUSION AND SUGGESTION FOR FUTHER WORKS</b>	170
7.1 Conclusion	170
7.2 Suggestion for further works	172
<b>REFERENCES</b>	175
<b>APPENDIX I- LIST OF INTERNATIONAL AND NATIONAL CONFERENCES</b>	187
A. 1.1	187
A. 1.2	188
A. 1.3	189
A. 1.4	190
A. 1.5	191
A. 1.6	192
A. 1.7	193
<b>APPENDIX II- LIST OF OTHERS PUBLISHED CHITOSAN PAPERS</b>	194
A. 2.1	194
A. 2.2	195
A. 2.3	196
A. 2.4	197
A. 2.5	198

## LIST OF TABLES

		<b>Pages</b>
Table 1.1	Mechanical properties of Cs bio-composites with respect of different types of filler	3
Table 1.2	Thermal properties of the Cs bio-composites with corresponding $T_w$ , $T_g$ and $T_d$	4
Table 1.3	Swelling properties of the Cs bio-composites in correspond to the $Q_t$ (%) and $t$ (min)	5
Table 3.1	The general properties of Cs powder	12
Table 3.2	The general properties of BT, DPA and ODA	13
Table 3.3	The general properties of NMP, AcOH, methanol and chloroform	13
Table 3.4	The general properties of NaOH and $P_4O_{10}$	14
Table 3.5	The composition of buffer solution as corresponds to different pH	14
Table 4.1	The total yield values of the samples derived from theoretical mass and practical mass	39
Table 4.2	The FTIR characteristics of Cs and XCs (BTC, DPAC and ODAC) samples at the respective wavelength	41
Table 4.3	The $\omega$ (eV) and $\square$ (%) on the Cs, BTC, ODAC and DPAC samples derived from XPS analysis	56
Table 4.4	The $E_v$ and $C_v$ (%) values of Cs, BTC, ODAC and DPAC samples as corresponds to the C, H, N and O elements.	57
Table 4.5	The solubility analysis of Cs, BTC, ODAC and DPAC in various pH medium; pH 2 to 6 (acidic medium), pH 7 (neutral) and pH 8 to 12 (base medium)	66
Table 4.6	The TG analysis on $T_{c1}$ , $T_{c2}$ , $M_{L1}$ and $M_{L2}$ values of Cs and XCs (BTC, ODAC and DPAC) samples.	73
Table 4.7	The DSC analysis on $T_{cw}$ , $T_g$ , $T_{cd}$ , $\Delta H_w$ and $\Delta H_d$ values of Cs and XCs (BTC, ODAC and DPAC) samples.	80
Table 5.1	The TG analysis details on $T_{c1}$ , $T_{c2}$ , $M_{L1}$ and $M_{L2}$ values of Cs/BTC, Cs/ODAC and Cs/DPAC bio-composites at different content of filler (0 to 12 wt/v %)	125
Table 5.2	The DSC analysis details on $T_{cw}$ , $T_g$ , $T_{cd}$ , $\Delta H_w$ and $\Delta H_d$ values of Cs/BTC, Cs/ODAC and Cs/DPAC bio-composites at different content of filler (0 to 12 wt/v %)	131

## LIST OF FIGURES

		<b>Pages</b>
Figure 1.1	Chemical structure of Cs; consist of N-G and N-G <sub>acetyl</sub> unit	2
Figure 3.1	The glassware set up of (a) purification of raw materials (b) purification of organic solvents (c) synthesise of XCs and (d) purification of XCs	16
Figure 3.2	Mechanism of the acid digestion process	30
Figure 4.1a	General formation of XCs filler; BTC, ODAC and DPAC with difference cross linking agents (i) BT, (ii) ODA and (iii) DPA, respectively	37
Figure 4.1b	Formation of amide groups between NH <sub>2</sub> groups of Cs with the anhydride of AA cross linking agents	38
Figure 4.2a	FTIR spectra of Cs and XCs (BTC, DPAC and ODAC) samples at wavelength of 4000 to 400 cm <sup>-1</sup> .	40
Figure 4.2b	The calculated DD values based on A <sub>1655</sub> and A <sub>3450</sub> peaks of Cs, BTC, ODAC and DPAC samples.	45
Figure 4.3	The <sup>1</sup> H NMR analysis of Cs and XCs (BTC, ODAC and DPAC) samples	47
Figure 4.4	The <sup>12</sup> C NMR analysis of Cs and XCs (BTC, ODAC and DPAC) samples	50
Figure 4.5a	The EDXS analysis of Cs, BTC, ODAC and DPAC samples within wide range of scan	54
Figure 4.5b	EDXS analysis of (a) Cs, (b) BTC, (c) ODAC and (d) DPAC samples at narrow signal of C 1s, O 1s and N 1s.	55
Figure 4.6	The ρ values of Cs and XCs (BTC, ODAC and DPAC) samples	59
Figure 4.7	Particle size analysis on (a) BTC, (b) ODAC and (c) DPAC samples	61
Figure 4.8	FESEM micrograph of Cs and XCs (BTC, ODAC and DPAC) samples at 500 X of magnification.	64

Figure 4.9	$W_a$ values of Cs and XCs (BTC, ODAC and DPAC) samples.	68
Figure 4.10	TG analysis of Cs and XCs (BTC, ODAC and DPAC) samples at (a) 35 to 500°C; (b) Ds1 and (c) Ds2	72
Figure 4.11	DSC analysis of Cs and XCs (BTC, DPAC and ODAC) samples at (a) Hs1 and (b) Hs2	78
Figure 5.1	The variation on viscosity and thickness of Cs/BTC, Cs/ODAC and Cs/DPAC bio-composites with the respect to different filler contents.	88
Figure 5.2	FESEM micrograph of Cs/ODAC bio-composites at different content of ODAC filler (a) 4 wt/v %; (b) 8 wt/v % and (c) 12 wt/v %	94
Figure 5.3	The $\sigma$ (MPa) versus $\varepsilon$ curves of (a) Cs/ODAC composites and (b) Cs/DPAC bio-composites at different content of filler. (i) the completed $\sigma$ versus $\varepsilon$ curves (ii) the elastic region of $\sigma$ over $\varepsilon$ curves	96
Figure 5.4	Variation on the $\sigma_R$ (MPa); $\varepsilon_R$ , K (MPa) and E (MPa) values of the Cs/BTC, Cs/ODAC and Cs/DPAC bio-composites at different content of filler.	99
Figure 5.5	The F (kN) versus D (mm) curves of (a) Cs/ODAC bio-composites and (b) Cs/DPAC bio-composites at different content of filler.	104
Figure 5.6	Variation on the F (kN) and D (mm) values of the Cs/BTC, Cs/ODAC and Cs/DPAC bio-composites at different content of filler.	105
Figure 5.7	The fracture surface of Cs/ODAC bio-composites under tension mode at different content of filler (a) 0ODAC, (b) 6ODAC, (c) 10ODAC and (d) 12 ODAC	113
Figure 5.8	The fracture surface of Cs/ODAC bio-composites under tearing mode at different content of filler (a) 0ODAC, (b) 6ODAC, (c) 10ODAC and (d) 12 ODAC	118
Figure 5.9	The fracture surface of Cs/DPAC bio-composites under tearing mode at different content of filler (a) 0DPAC, (b) 6DPAC, (c) 8DPAC and (d) 12DPAC	120
Figure 5.10	TG analysis thermograph of the (a) Cs/ODAC bio-composites and (b) Cs/DPAC bio-composites with different filler content at analyzed temperature of (i) 30 to 500 °C;	123

	(ii) 70 to 120 °C and (iii) 280 to 300 °C	
Figure 5.11	Derivative TG thermograph of the (a) Cs/ODAC bio-composites and (b) Cs/DPAC bio-composites with different filler content at analyzed temperature of (i) 30 to 500 °C ; (ii) 70 to 120 °C and (iii) 220 to 350 °C	124
Figure 5.12	DSC thermographs of $T_w$ for (a) Cs/BTC bio-composites, (b) Cs/ODAC bio-composites and (c) Cs/DPAC bio-composites at different content of ODAC filler for the Hs1 (35 to 150 °C)	128
Figure 5.13	DSC thermographs of $T_g$ and $T_d$ for the (a) Cs/BTC bio-composites, (b) Cs/ODAC bio-composites and (c) Cs/DPAC bio-composites at different content of filler for the Hs2 (-50 to 500 °C)	130
Figure 5.14	Response of DM Analysis on $E'$ (MPa) of the (a) Cs/BTC bio-composites, (b) Cs/ODAC bio-composites and (c) Cs/DPAC bio-composites at different content of filler	135
Figure 5.15	Response of DM Analysis on $\tan \delta$ of the (a) Cs/BTC bio-composites, (b) Cs/ODAC bio-composites and (c) Cs/DPAC bio-composites	136
Figure 5.16	An overview on (a) $T_{c1}$ and (b) $T_{c2}$ of Cs/BTC bio-composites, Cs/ODAC bio-composites and Cs/DPAC bio-composites.	139
Figure 5.17	Variation of $T_g$ (°C) on filler content of the Cs/BTC, Cs/ODAC and Cs/DPAC bio-composites.	140
Figure 5.18	An overview on $T_g$ values derived from (a) $E'$ (b) $E''$ and (c) $\tan \delta$ of the Cs/BTC bio-composites, Cs/ODAC bio-composites and Cs/DPAC bio-composites	142
Figure 5.19	The $Q_t$ over $t$ curves of Cs/ODAC bio-composites film varies content of filler (0 to 12 wt/v%) and at different pH of swollen medium (a) pH 2; (b) pH 4 and (c) pH 6	144
Figure 5.20	The $Q_t$ over $t$ curves of Cs/DPAC bio-composites film varies content of filler (0 to 12 wt/v%) and at different pH of swollen medium (a) pH 2; (b) pH 4 and (c) pH 6	146
Figure 5.21	The overview on $Q_t$ (%), $t$ (days) and $Q_r$ (% min <sup>-1</sup> ) of the (a) Cs/BTC bio-composites, (b) Cs/ODAC bio-composites and (c) Cs/DPAC bio-composites at different content of filler	148

Figure 5.22	The proposed protonization mechanism of (a) $\text{NH}_2$ groups (b) $\text{NHCH}_2\text{OH}$ and (c) diisociation of $\beta$ -glycosidic linkage of Cs matrix in swollen acidic medium	149
Figure 5.23	The proposed diisociation of NH-R linkage of (a) ODAC filler and (b) DPAC filler in swollen acidic medium	150
Figure 5.24a	The $Q_t$ over $t$ curves of (a) Cs/ODAC composites film (b) Cs/DPAC composites film with varies content of filler (0 to 12 wt/v%) in swollen medium of pH 7	151
Figure 5.24b	The overview on $Q_t$ , $t$ and $Q_r$ values of Cs/BTC, Cs/ODAC and Cs/DPAC bio-composites in neutral swollen medium (pH7)	152
Figure 5.25	The proposed inter hydrogen bonds of (a) Cs matrix (b) ODAC filler and (c) DPAC filler with $\text{H}_2\text{O}$ molecules	154
Figure 5.26	The $Q_t$ over $t$ curves of Cs/ODAC bio-composites at varies content of filler (0 to 12 wt/v%) and in different pH of swollen medium (a) pH 8; (b) pH 10 and (c) pH 12	156
Figure 5.27	The $Q_t$ over $t$ curves of Cs/DPAC bio-composites at varies content of filler (0 to 12 wt/v%) and in different pH of swollen medium (a) pH 8; (b) pH 10 and (c) pH 12	158
Figure 5.28	The overview on $Q_t$ , $t$ and $Q_r$ values of Cs/BTC, Cs/ODAC and Cs/DPAC bio-composites in various alkaline medium; (a) pH 8, (b) pH 10 and (c) pH 12	159
Figure 5.29	The proposed hydrolysis linkage of $\text{NHCOCH}_3$ groups of Cs matrix in alkaline medium	160

## LIST OF SYMBOLS

$\delta$	Particle size
$\Delta H$	Heat fusion
$\Delta H_{de}$	Heat fusion of degradation peak
$\Delta H_w$	Heat fusion of evaporation peak
$A_{1655}$	Transmitted intensity at 1655 $\text{cm}^{-1}$
$A_{3450}$	Transmitted intensity at 3450 $\text{cm}^{-1}$
C	Carbon element
C=O	Carbonyl group
C1	First carbon of Cs ring
C2	Second carbon of Cs ring
C3	Third carbon of Cs ring
C4	Fourth carbon of Cs ring
C5	Fifth carbon of Cs ring
COOH	Carboxylic groups
$C_D$	Completely dissolved
Cr	Crystalline level
$C_v$	Calculated values
D	Optimum deformation
Ds1	First decomposition stage
Ds2	Second decomposition stage
E	Tensile modulus
$E'$	Storage modulus
$E''$	Loss modulus
$E_v$	Experimental values
F	Optimum force
$G_{acetyl}$	2-amino-2-deoxy- $\beta$ -D-acetylglucopyranose
$G_{amide}$	2-amide-2-deoxy- $\beta$ -D-glucopyranose
$G_{amine}$	2-amino-2-deoxy- $\beta$ -D-glucopyranose

H	Hydrogen element
H <sup>+</sup>	Hydroion
H <sub>2</sub> O	Water molecules
Hs1	First heating scan
Hs2	Second heating scan
I <sub>020</sub>	Maximum intensity at $\approx 12^\circ$
I <sub>110</sub>	Maximum intensity at $\approx 20^\circ$
I <sub>am</sub>	Intensity of amorphous diffraction at $16^\circ$
K	Tensile toughness
M <sub>f</sub>	Final mass
M <sub>L</sub>	Mass loss
M <sub>L1</sub>	Mass loss of Ds1
M <sub>L2</sub>	Mass loss of Ds2
M <sub>Lr1</sub>	Mass loss of T <sub>r1</sub>
M <sub>Lr2</sub>	Mass loss of T <sub>r2</sub>
M <sub>s</sub>	Starting mass
M <sub>w</sub>	Molecular weight
N	Nitrogen element
N <sub>D</sub>	Not dissolved
NH <sub>2</sub>	Primary amine group
NH <sub>3</sub> <sup>+</sup>	Cationic primary amine group
O	Oxygen element
OH <sup>-</sup>	Hydroxyl ion
P <sub>D</sub>	Partially dissolved
Q <sub>r</sub>	Rate of swelling
Q <sub>t</sub>	Degree of swelling
rpm	Rotation per minute
SMC	Spindle constant
t	Time of equilibrium swelling
tan $\delta$	tan deltha
T <sub>c</sub>	Midpoint



$T_{c1}$	Midpoint temperature of Ds1
$T_{c2}$	Midpoint temperature of Ds2
$T_d$	Degradation temperature
$T_g$	Glass transition temperature
TK	Torque constant
$T_{r1}$	Reference temperature of Ds1
$T_{r2}$	Reference temperature of Ds2
$T_w$	Evaporation temperature
$W_a$	Water adsorption
$W_a$	Adsorption ability
$W_{dry}$	Weight dry of samples
$W_{wet}$	Weight wet of samples
$\square$	Portion of an element
$\epsilon_R$	Tensile strain
P	Bulk density
$\sigma_R$	Tensile strength
$\Omega$	Bonding energy

## LIST OF ABBREVIATIONS

$^1\text{H}$ NMR	$^1\text{H}$ Nuclear Magnetic Resonance
$^{12}\text{C}$ NMR	$^{12}\text{C}$ Nuclear Magnetic Resonance
AA	Acid anhydride
AcOH	Acetic acid
BC	Bamboo charcoal
BT	1,2,4,5-benzotetra carboxylic
BTC	1,2,4,5-benzotetra carboxylic-chitosan
CG	Cashew gum
CMC	Carboxymethyl cellulose
Cs	Chitosan
CW	Cellulose whiskers
DD	Degree of deacetylation
DM	Dynamic Mechanical
DPA	3,3',4,4'-diphtalic anhydride
DPAC	3,3',4,4'-diphtalic anhydride-chitosan
DSC	Differential Scanning Calorimetry
EDXS	Energy Dispersive X-ray Spectroscopy
FESEM	Fields Emission Scanning Electron Microscope
FTIR	Fourier Transform Infra Red
GAA	Glycial acetic acid
HA	Hydroxyapatite
HDI	Hexamethylene diisoyanate
HEPK	2-hydroxyl-1-[4-(2-hydroxyethoxy)phenyl]-2-methyl-1-propanone
KD	Kenaf dust
MC	Methylcellulose

MNC	Micro/nano clay
MWCNTs	Multiwall carbon nanotube
NaHCO <sub>3</sub>	Sodium alginate
NMP	N-methyl pyrrolidone
OA	Oleic acid
ODA	4,4'-oxydiphtalic anhydride
ODAC	4,4'-oxydiphtalic anhydride-chitosan
PAAA	Poly(acrylic acid-co-acrylamide)
PCL	Polycaprolactone
PEG	Polyethylene glycol
PEGDMA	Poly(ethyleneglycol)-600-dimethylcylate
PP	Potassium persulfate
QPVP	Quarternized poly(4-vinyl-N-carboxymethyl pyridine)
TG	Tamarind gum
TG	Thermogravimetry
TPP	Tripolyphosphate
XCs	Cross linked chitosan
XRD	X-ray diffraction

## **PENGHASILAN DAN PENCIRIAN CHITOSAN TERSAMBUNG SILANG**

### **TERISI CHITOSAN KOMPOSIT**

#### **ABSTRAK**

Ikatan antara muka, keseragaman dan kekakuan pengisi adalah ciri-ciri utama yang mempengaruhi sifat-sifat mekanikal, haba dan hidrofilik bio-komposit chitosan (Cs). Oleh itu, tujuan kajian ini adalah untuk mengkaji peranan chitosan tersambung silang (XCs) sebagai pengisi di dalam matrik Cs terhadap kualiti antara muka, keseragaman dan kekakuan bio-komposit Cs. Pengisi XCs dihasilkan menggunakan tiga agen tersambung silang berlainan iaitu *1,2,4,5-benzentetra carboxylic* (BT), *4,4'-oxydiphtalic anhydride* (ODA) dan *3,3',4,4'-diphthalic anhydride* (DPA) yang menghasilkan tiga jenis pengisi XCs: *1,2,4,5-benzentetra carboxylic-chitosan* (BTC), *4,4'-oxydiphtalic anhydride-chitosan* (ODAC) dan *3,3',4,4'-diphthalic anhydride-chitosan* (DPAC). Pembentukan struktur amida (sebagai jambatan tersambung silang) dibuktikan melalui analisa kimia, fizikal dan haba menggunakan pengubah fourier infra merah (FTIR),  $^1\text{H}$  dan  $^{12}\text{C}$  resonansi kemagnetan nuklear ( $^1\text{H}$  and  $^{12}\text{C}$ NMR), penganalisis elemen, tenaga serakan sinar x-ray spektroskopi (EDXS), pembelauan sinar x-ray (XRD), saiz partikel, ketumpatan, graviti permeteran haba (TG), pembeza pengimbas kalorimetri (DSC), Mikroskopi lapangan emisi pengimbas elektron (FESEM), ujian keterlarutan dan pengembangan. Teknik pengacuan larutan kemudiannya digunakan untuk menghasilkan bio-komposit Cs/XCs dengan kandungan pengisi 0 hingga 12 wt/v%. Sifat-sifat mekanikal (berdasarkan ujian tegangan dan koyakkan), haba (berdasarkan analisa TG,

DSC dan analisa dinamik mekanikal (DMA)) dan hidrofilik (menggunakan larutan pH 2 hingga 12) bio-komposit kemudiannya dianalisa. Didapati kekuatan tegangan ( $\sigma_R$ ), modulus tegangan (E) dan daya ketahanan (F) Cs meningkat dari 66.7 hingga 421.3 % dengan penambahan 2 hingga 10 wt/v% pengisi XCs. Sementara itu, nilai regangan tegangan ( $\epsilon_R$ ), keliatan (K) dan pemanjangan (D) menurun 65.1 hingga 72.1 % pada kandungan pengisi yang sama. Kesan penambahan pengisi XCs (2 hingga 10 wt/v%) terhadap sifat-sifat haba Cs diperolehi apabila suhu peralihan kacanya ( $T_g$ ) meningkat pada kadar purata 2.5 % pada setiap penambahan 2 wt/v% pengisi. Selanjutnya, nilai pengembangan ( $Q_t$ ), kadar pengembangan ( $Q_r$ ) dan masa pengembangan (t) Cs di dalam semua larutan pH menurun sebanyak 5.2 hingga 70.3 % dengan penambahan 2 hingga 10 wt/v% pengisi XCs. Diantara semua bio-komposit yang dihasilkan, Cs/DPAC mempamerkan sifat-sifat mekanikal, haba dan rintangan hidrophilik yang terbaik diikuti dengan bio-komposit Cs/BTC dan Cs/ODAC. Keputusan-keputusan di atas adalah dipengaruhi oleh sifat antara muka dan keseragaman yang baik antara matrik Cs dan pengisi XCs melalui pembentukan ikatan hidrogen dan interaksi elektrostatik. Kehadiran kedua-duanya dibuktikan secara analisa kimia dan mikroskopik. Selain itu, sifat kekakuan bio-komposit Cs/XCs terhasil daripada struktur tersambung silang pengisi XCs.

# **PREPARATION AND CHARACTERIZATION OF CROSS LINKED CHITOSAN FILLED CHITOSAN COMPOSITES**

## **ABSTRACT**

The interfacial bonds, homogeneity and rigidity of filler are the two main criteria that significantly influenced the mechanical, thermal and hydrophilicity of the chitosan (Cs) based bio-composites. Therefore, the aim of this study was to investigate the role of cross linked chitosan (XCs) as filler in the Cs matrix towards the interfacial, homogeneity and rigidity of the produced Cs bio-composites. XCs was synthesized using three different cross linking agents named as 1,2,4,5-benzenetra carboxylic (BT), 4,4'-oxydiphthalic anhydride (ODA) and 3,3',4,4'-diphthalic anhydride (DPA) which consequently produced three different types of XCs filler; 1,2,4,5-benzenetra carboxylic-chitosan (BTC), 4,4'-oxydiphthalic anhydride-chitosan (ODAC) and 3,3',4,4'-diphthalic anhydride-chitosan (DPAC). The formation amide structure (as the cross linking bridge) was chemically, physically and thermally prove via the Fourier Transform Infra-Red (FTIR),  $^1\text{H}$  and  $^{12}\text{C}$  Nuclear Magnetic Resonance ( $^1\text{H}$  and  $^{12}\text{C}$ NMR), elemental analysis, Energy Dispersive X-ray Spectroscopy (EDXS), X-ray diffraction (XRD), particle size analysis, density, Thermogravimetry (TG), Differential Scanning Calorimetry (DSC), Field Emission Scanning Electron Microscope (FESEM), solubility and swelling analysis. The solution casting technique was used to fabricate the Cs/XCs bio-composites with the filler content of 0 to 12 wt/v %. The properties of the produced bio-composites were analyzed on its mechanical (under tensile and tearing testing), thermal (TG, DSC and Dynamic Mechanical (DM) analysis) and hydrophilicity properties (under swollen medium of pH 2 to 12). It was found that the tensile strength

( $\sigma_R$ ), tensile modulus (E) and force (F) of neat Cs film increased almost 66.7 to 421.3 % with addition of 2 to 10 wt/v % of the XCs filler. While, the tensile strain ( $\epsilon_R$ ), toughness (K) and deformation (D) values of the bio-composites reduced 65.1 to 72.1 % in correspond to the similar content of the fillers. Effect of the addition of XCs filler (2 to 10 wt/v %) towards thermal properties of the neat Cs film was observed as its glass transition temperature ( $T_g$ ) value increased with average of 2.5% for each of 2 wt/v %. Furthermore, the degree of swelling (Qt) rate of and swelling (Qr) of neat Cs film in all examined pH medium was reduced 5.2 to 70.3 % with the incorporation of 2 to 10 wt/v % of XCs filler. Of all produced bio-composites, Cs/DPAC bio-composites showed the most superior mechanical, thermal and hydrophobic properties followed by Cs/BTC and Cs/ODAC bio-composites. The above results were influenced by the good interfacial bonds and homogeneity between the Cs matrix and XCs filler which brought by inter hydrogen bonds and electrostatic interactions. Both of the interactions were chemically and microscopically revealed. Besides, the properties of the bio-composites was also credited by the rigidity of the XCs filler through its cross linked structure.

## CHAPTER 1

### INTRODUCTION

#### 1.0 Overview

The first part of the chapter reviews the current status, the research gap, and the potential, as well as the applications of Cs (Chitosan) bio-composite. Consequently, the limitations of the bio-composites regarding compatibility, homogeneity, and rigidity was highlighted, in terms of mechanical, thermal and swelling properties. Thus, the new types of cross linked Cs (XCs) filler were proposed and several hypotheses on its performances towards Cs bio-composites were discussed. The chapter ended with five main objectives of the study.

#### 1.1 Cs bio-composites

Currently, the increasing cost of petroleum and the ever-increasing pollution from non-degraded synthetic polymers have directly threatened human being's survival, health and development. Therefore, bio-degradable polymers from renewable resources have attracted considerable attention for sustainable development and environmental preservation. Cs a copolymer of 2-amino-2-deoxy- $\beta$ -D-glucopyranose ( $G_{\text{amine}}$ ) and 2-amino-2-deoxy- $\beta$ -D-acetylglucopyranose ( $G_{\text{acetyl}}$ ) (Figure 1.1), is the deacetylated derivative of chitin and one of the most plentiful and attractive bio-polymers (Li *et al.*, 2010)



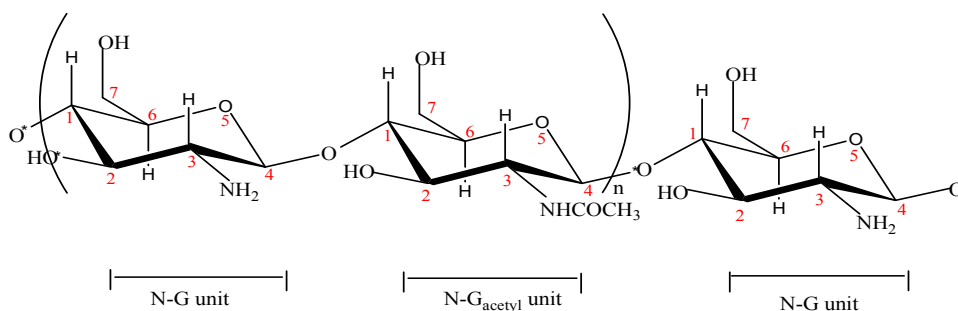


**Figure 1.1:** Chemical structure of Cs; consist of N-G<sub>amine</sub> and G<sub>acyetyl</sub> unit

Owing to its specific structure and properties, Cs has attracted significant interest in a broad range of applications such as witnessed in biomedical, biosensor, cosmetic, biotechnology, food industry, agriculture, paper industry and environmental protection (Qin *et al.*, 2007). However, the use of Cs films has been largely restricted due to their inherent water (H<sub>2</sub>O) sensitivity easily degrade and relatively weak in mechanical and thermal properties as compared to most of the synthetic polymers (Diez-Sales *et al.*, 2007).

Thus, it is of interest to incorporate the Cs polymer with filler and produced Cs bio-composites. Cs bio-composites have a potential to be used for applications like bio-sensor, medical surgical, coating, packaging, and waste water treatments (Khunawattanakul *et al.*, 2011). Currently, several organic and synthetic fillers are available for the Cs bio-composites including metal based, metal oxide ions based, metal oxide based, ceramic based, mineral based, cellulose based, polysaccharide based, natural fiber, rubber based, carbon fiber, protein based and carbon nano based (Spinks *et al.*, 2005).

Numerous studies have demonstrated the addition of the filler gave a positive response in strength and modulus while limiting the extensibility and deformation of the Cs bio-composites (Table 1.1).

**Table 1.1:** Mechanical properties of Cs bio-composites with respect of different types of filler with corresponded to the tensile strength ( $\sigma_R$ ), tensile strain ( $\epsilon_R$ ) and tensile modulus (E)

Types of Cs	$\sigma_R$ (MPa)	$\epsilon_R$ (%)	E(MPa)	References
2 % chitosan film	39.47 $\pm 6.6$	37.44 $\pm 2.9$	-	Miranda <i>et al.</i> , (2004)
2 % chitosan + 0.3 % PEG	14.57 $\pm 1.7$	49.56 $\pm 3.1$	-	Miranda <i>et al.</i> , (2004)
2 % chitosan + 0.3 % sorbiol	38.48 $\pm 3.3$	56.91 $\pm 4.2$	-	Miranda <i>et al.</i> , (2004)
2 % chitosan + 0.6 % glycerol	33.69 $\pm 3.7$	167 $\pm 3.6$	-	Miranda <i>et al.</i> , (2004)
Chitosan + collagen	1.19 $\pm 0.4$	-	39.78 $\pm 5.60$	Kai <i>et al.</i> , (2004)
Chitosan + collagen + HA	21.88 $\pm 3.21$	-	1159.5 $\pm 79.1$	Kai <i>et al.</i> , (2004)
Chitosan + 30 wt % CMC	3.5	-	-	Jiang <i>et al.</i> , (2008)
Chitosan film	75	2.6	5000	Nitayaphat <i>et al.</i> , (2009)
Chitosan + 1 wt % BC	110	2.8	7000	Nitayaphat <i>et al.</i> , (2009)
2 % chitosan film	82 $\pm 15$	4 $\pm 3.2$	-	Casariego <i>et al.</i> , (2009)
2 % chitosan + 3 w/w % MNC	60 $\pm 10$	6 $\pm 0.5$	-	Casariego <i>et al.</i> , (2009)
Chitosan film	39.6 $\pm 3.2$	15.2 $\pm 1.2$	200.1 $\pm 0.12$	Coa <i>et al.</i> , (2009)
Chitosan +0.2 % MWCNTs	102.8 $\pm 3.6$	7.9 $\pm 1.1$	435 $\pm 0.26$	Coa <i>et al.</i> , (2009)
Chitosan film	85	20	-	Li <i>et al.</i> , (2009)
Chitosan + 20 wt % CW	120	6	-	Li <i>et al.</i> , (2009)
Chitosan film	12	17	310	Vargas <i>et al.</i> , (2004)
Chitosan + 1 v/w % OA	18	15	495	Vargas <i>et al.</i> , (2004)
Chitosan film	2	62	-	Joseph <i>et al.</i> , (2009)
Chitosan + 25 % PCL	6.2	35	-	Joseph <i>et al.</i> , (2009)
Chitosan film	25.99 $\pm 2.97$	28.15 $\pm 6.15$	-	Joseph <i>et al.</i> , (2009)
Chitosan + 90 % v PCL	24.75 $\pm 4.01$	28.69 $\pm 4.32$	-	Joseph <i>et al.</i> , (2009)
Chitosan film	27	32	-	Xu <i>et al.</i> , (2005)
50 % Chitosan + 50 % starch	40	52	-	Xu <i>et al.</i> , (2005)
Chitosan film	62	11.8	-	Sriupoyo <i>et al.</i> , (2005)

*Continue:*

Types of Cs	$\sigma_R$ (MPa)	$\epsilon_R$ (%)	E(MPa)	References
Chitosan + 2.95 wt % $\alpha$ CW	80	8	-	Sriupoyo <i>et al.</i> , (2005)
Chitosan film	-	4	3000	Garcia <i>et al.</i> , (2005)
25 % chitosan + 75 % MC	-	8	1600	Garcia <i>et al.</i> , (2005)

PEG = Polyethylene glycol  
CMC = Carboxymethyl cellulose  
MNC = Micro/nano clay  
CW = Cellulose whiskers  
PCL = Polycaprolactone  
MC = Methyl cellulose

HA = Hydroapatite  
BC = Bamboo charcoal  
MWCNTs = Multi wall carbon nano tube  
OA = Oleic acid  
 $\alpha$ -CW =  $\alpha$ -chitin whisker

Generally, strength of neat Cs films is 38 to 66 MPa; approximately twice than the polyethylene (Qin, 2008). Furthermore, this value is generally increased with the addition on various types of filler. Table 1.1 demonstrated the potential of the filler to develop the barrier of energy transfer of the Cs bio-composites during the mechanical testing. The reinforcement effect induced by the filler is illustrated by the crack propagation of the bio-composites during the testing (Spinks *et al.*, 2005).

For more than 20 years researchers have focused on the effect of addition of the filler toward the thermal properties of Cs bio-composites (Table 1.2). Cs polymer poses a disadvantage since it is thermally degraded appreciably at low heating temperature (200 to 300 °C) (Hong *et al.*, 2007). During the degradation, the polysaccharide linkage of Cs polymer is progressively split and breaks that result in the reduction on most of its thermal properties.

**Table 1.2:** Thermal properties of the Cs bio-composites with correspond to the dehydration temperature ( $T_w$ ), glass transition temperature ( $T_g$ ) and degradation temperature ( $T_d$ )

Types of Cs	$T_w$ (°C)	$T_g$ (°C)	$T_d$ (°C)	References
Cs film	46	-	256	Maciel <i>et al.</i> , (2005)
Cs +CG	52	-	242	Maciel <i>et al.</i> , (2005)
Cs + Collagen	95	-	-	Tsai <i>et al.</i> , (2007)
Cs + alginate	155	130	250	Mladenovska <i>et al.</i> , (2007)

*Continue:*

Types of Cs	T <sub>w</sub> (°C)	T <sub>g</sub> (°C)	T <sub>d</sub> (°C)	References
Cs film	-	-	200	Zhang <i>et al.</i> , (2007)
Cs + TG	-	-	307	Zhang <i>et al.</i> , (2007)
Cs + Kollicoat	-	50	-	Wei <i>et al.</i> , (2009)
Cs film	-	-	232	Moura <i>et al.</i> , (2007)
Cs + HPM	-	-	271	Moura <i>et al.</i> , (2007)

TG= Tamarind gum

HPM= Hydropropyl methyl cellulose

CG=Cashew gum

The previous data in Table 1.2 interpreted that addition of rigid filler restricted the molecular chains, transition phase, heat distortion temperature and degradation of the Cs bio-composites during the thermal analysis.

The Cs bio-composites are also attracting widespread interest for its hydrophilic properties (Table 1.3). Due to the abundant of polar groups (OH, NH<sub>2</sub>, COOH and NH-R) with the semi crystalline nature, Cs polymers tend to absorb the surrounding moisture.

**Table 1.3:** Swelling properties of the Cs bio-composites with correspond to the degree of swelling (Qt) and duration to reach equilibrium state (t)

Types of Cs	Qt(%)	t (min)	References
Cs + 61% PEG	2700	140	Kuichi <i>et al.</i> , (2008)
Cs film	750	-	Chuang <i>et al.</i> , (2008)
Cs + PP + AA	1250	-	Chuang <i>et al.</i> , (2008)
Cs + 50 % QPVP	75	-	Casariago <i>et al.</i> , (2009)
Cs dipping into NO <sub>2</sub> GAA	110	420	Phisalaphong <i>et al.</i> , (2008)
Cs film	115	1440	Liu <i>et al.</i> , (2007)
Cs + 0.6 % NaHCO <sub>3</sub>	740	1440	Liu <i>et al.</i> , (2007)
Cs + 70 wt% collagen	85	-	Yang <i>et al.</i> , (2007)
Cs + 70 wt % collagen + 0.7wt% heparin	100	-	Yang <i>et al.</i> , (2007)
Cs film	9000	1440	Ma <i>et al.</i> , (2007)
Cs + 5% glycerol	1500	1440	Ma <i>et al.</i> , (2007)
Cs + 50 % PEGDMA + HEPK	8000	1440	Wang <i>et al.</i> , (2008)
3 % Cs + 10 % TPP	45	120	Guan <i>et al.</i> , (2007)
Cs + PVA + glycerol	3000	4320	Jin <i>et al.</i> , (2008)
Cs + PAAA	13000	240	Rayment <i>et al.</i> , (2008)
Cs film	350	180	Yang <i>et al.</i> , (2008)

*Continue:*

<b>Types of Cs</b>	<b>Qt(%)</b>	<b>t (min)</b>	<b>References</b>
Cs + Starch	370	180	Yang <i>et al.</i> , (2008)
Cs + Clay	380	180	Yang <i>et al.</i> , (2008)
Cs + 0.25 wt % HDI + 50 wt % ethanol	60.2	2880	Yin <i>et al.</i> , (2008)
Cs + 5wt% CW	68	-	Sangeetha & Abraham, (2008)

PEG = Polyethylene glycol	PP = Pottosium persulfate
AA = Acrylic acid	QPVP = Quarternized poly(4-vinyl-N-carboxymethyl)
GAA = Glycial acetic acid	NaHCO <sub>3</sub> = Sodium alginate
PEGDMA = Poly(ethyleneglycol)-600-dimethylcylate	HEPK = 2-hydroxyl-1-[4-(2-hydroxyethoxy)
TPP = Tripolyphosphate	PAAA = Poly(acrylic acid-co-acrylamide)
HDI = Hexamethylene diisoyanate	CW = Cellulose whiskers

Peirano *et al.*, (2008) have pointed out Cs is highly permeable for H<sub>2</sub>O molecules, soluble and degraded in acidic medium and shrinkage in alkaline medium. Thus, addition of filler results in the reduction on hydrophilic properties of Cs film over all pH medium (Nitayaphat *et al.*, 2009). The hydrophobicity, bulky and high molecular weight ( $M_w$ ) properties of the filler limits the adsorption and swelling mechanism of the Cs film. The limitation occurred as the filler formed a protective barrier to hide the polar groups of the Cs polymer.

## 1.2 Problem statements

The limitations of Cs bio-composites have been addressed regarding compatibility, homogeneity and rigidity of the filler in Cs matrix. The combination of the filler and Cs matrix normally results in incompatibility. The incompatibility of the bio-composites derived from a weak interaction between filler and matrix. Most of the filler is not compatible with Cs matrix, since only mechanical and physical interactions such as interlocking, gripping, Van da Waals, dipole-dipole interactions, inter hydrogen bonds, acid base interactions and polar interactions occurred at the

interfacial area. The interactions are relatively weak as compared to the chemical interactions.

The incompatibility of Cs bio-composites was also demonstrated under thermal analysis. For example, addition of hydroxyapatite (HA) filler into Cs matrix resulted into un-identical thermograph curves between the Cs/HA bio-composites, HA filler and neat Cs film (Chen *et al.*, 2007). The combination of Cs matrix with zeolite filler showed three-stage decomposition instead of only two stages by neat Cs film (Sun *et al.*, 2008). Two series of  $T_g$  peaks observed as Cs matrix combined with 2 % (v/v) of poly (ethylene oxide) (Neto *et al.*, 2005). Meanwhile, addition of 6 % tamarind gum into Cs matrix split the  $T_d$  of the bio-composites into two; 285 and 425 °C, respectively (Huang *et al.*, 2005).

Another limitation of Cs bio-composites is to establish homogenous filler dispersion in the Cs matrix. Basically, the bio-composites with excellent properties supplied with a well-distribute filler over the polymer matrix. However, a homogenous dispersion of filler in Cs matrix is often difficult to achieve, due to the differences in sources, physical properties (density, phases and shape) and chemical properties ( $M_w$ , solubility, functional groups, configuration and reactivity) between both components.

Moreover, the rigidity of filler also plays an important role to produce Cs bio-composites with good reinforcement effects. Generally, the organic filler is relatively less rigid than synthetic ones. However, despite of costly production, the synthetic filler scarified most on bio-compatibility, bio-activity and bio-degradability properties of the Cs film. Ma *et al.*, (2007) prepared the Cs/alginate bio-composites

and pointed out that the reinforcing and toughening effects of the bio-composites were primarily attributed by the rigidity of filler.

Meanwhile, cross linking is another approach that has been proven to significantly increase the performance of Cs film. The cross linked Cs (XCs) supplied with rigid, integrated and strong structure (Rayment *et al.*, 2008) as compared to linear Cs. This is necessary to reduce the deformation, alignment, toughness and crystallinity, while increased the elasticity and strength of the Cs film. Therefore, the rigid structure of XCs increased the thermal stability of Cs polymer. Close examination on the thermograph of linear Cs and XCs by Kumari *et al.*, (2008) and Ou *et al.*, (2008) reveal the differences  $T_w$  and  $\Delta H_w$  values and concluded that XCs has better resistance to H<sub>2</sub>O content as compared to neat Cs. Devi *et al.*, (2005) have pointed out the  $T_g$  of Cs that generally occurred at 112 °C has been altered to 177 °C for XCs. Such alteration is attributed to the formation of stronger inter chemical bonds (covalent bonds) within the XCs molecules.

Cross linking also lowered the hydrophilicity by improving the surface hydrophobicity and chains resistance of the Cs polymers. The cross linked structure restrict the extensibility of XCs polymer chains and block the polar groups of XCs that in turn, more inert and hydrophobic structure is obtained (Argin-Soysal *et al.*, 2009). Wang *et al.*, (2008) found the linear relationship of H<sub>2</sub>O contact angle with the cross linking degree of XCs.

With the above factors, various cross linking agents such as aldehyde based, amino acids based, peroxide based, glycol based, ether based, isocyanate based and acrylate based were utilized for XCs production. Of these cross linking agents, acid anhydride based (AA) cross linking agents offer insignificant violently reaction with

more gentle warming cross linking process as compared to others (Huang *et al.*, 2008). Additionally, the COOH groups of AA preferentially react with NH<sub>2</sub> than OH; thus avoiding undesirable reaction. The aromatic structure supplied AA cross linking agents with thermally stable and more rigid as compared to other common aliphatic cross linking agents.

However, the formation of cross linked structure limits the solubility and film forming ability of XCs (Vondran *et al.*, 2008). The limitation is brought by the reduction on number of polar groups and restriction of Cs polymer chains. Alternatively, to produce cross linked Cs film; the XCs are used as a filler to reinforce the Cs matrix.

### **1.3 Hypothesis of Cs/XCs bio-composites**

The extraordinary mechanical, thermal and resistance properties of the XCs make them out standing filler to be incorporated with Cs matrix. The similarity in polymer chains of XCs filler and Cs matrix induced a better compatibility between both of components. Due to the numerous functional groups (OH, COOH, NH-R, C-N and C-O-C), XCs will establish more inter molecular interactions with the Cs matrix. Regardless of the conditions and parameters of testing, both of XCs filler and Cs matrix will result in similar responses. This consequently, reduced constrain on the effect of the interfacial regions of the bio-composites.

The homogeneity of XCs filler distribution in Cs matrix will be achieved due to the solubility of the filler. Since both of XCs and Cs molecular derived from the similar sources, the XCs filler could be easily mixed into the similar procedures of



Cs matrix. The mixing process will produce the bio-composites mixture with minimum precipitation, agglomeration and phase separation; yielding more homogenous mixture.

From the engineering point of, the rigidity of XCS filler is supplied by its cross linked, aromatic and bulky structure. The cross linked structure of XCs will anchor the linear structure of Cs matrix thus; greater level of energy is needed to destroy the bio-composites structure. The bulky groups of XCs will create a batter barrier for the adsorption process. Consequently, the swelling mechanism of the Cs/XCs bio-composites is minimized, stabilized and controllable.

#### **1.4 Objectives of research**

The primary objectives of the study are:

- 1- To synthesize the XCs filler using three different AA cross linking agents.
- 2- To characterize the physical, chemical and thermal properties of XCs filler.
- 3- To fabricate and optimize the preparation parameters of Cs/XCs bio-composites with different types and content of XCs filler
- 4- To study the effect on compatibility, homogeneity and rigidity of XCs filler into Cs matrix through the chemical interactions, mechanical, thermal and swelling properties of the Cs/XCs bio-composites
- 5- To optimize the mechanical, thermal and swelling properties of all types Cs/XCs bio-composites.

## CHAPTER 2

### LITERATURE REVIEW

#### 2.0 Overview

The general views of preparation, application and current status of Cs bio-composites was given in the review paper entitle of “*The preparation, properties and applications of chitosan based bio-composites/blend materials- A review*” (Chapter 6; Paper I). The paper starts with the general introductions of Cs polymers with regards to its; occurrence, properties, advantages and limitations. Consequently, the significant effect of reinforcing and/or blending Cs polymer with the different constituents to increase various properties (mechanical, hydrophilic, thermal, adsorption ability and stability) has been discussed in details. It is concluded that the properties of Cs bio-composites with synthetic filler have contributed to its rigidity since only mechanical interaction occurred at the interfacial region. Instead of physical interactions, the addition of organic filler also promoted the chemical interactions at the interfacial region of the Cs bio-composites. This consequently produced Cs bio-composites with synthetic filler with relatively low strength and stiffness but high resistance to fracture, whereas the ones with organic filler have high strength and stiffness but are very brittle. This review also screens the current applications of Cs-based bio-composites in the field of drug delivery, tissue engineering, antibacterial, food packaging, biomedical, metal adsorption and dye removal.

## CHAPTER 3

### MATERIALS AND METHODOLOGY

#### 3.0 Overview

The chapter starts with list on description of materials, synthesis parameters and characterization on three types of XCs filler namely as the BTC, ODAC and DPAC. Preparation and testing methods of the Cs/XCs bio-composites were then discussed in the following sections.

#### 3.1 Materials

##### 3.1.1 Cs powder

Cs powder was purchased from Hunza Pharmaceutical (Malaysia) Sdn Bhd with the following properties (Table 3.1).

**Table 3.1:** The general properties of Cs powder

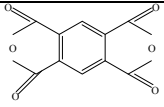
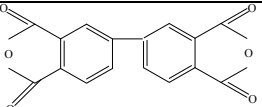
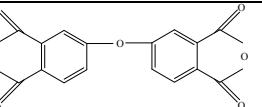
<b>Properties</b>	<b>Identification</b>
Grade	Pharmaceutical grade
Degree of deacylation	$\leq 92 \%$
Solubility in 1 % solution of 1 % AcOH	$\geq 98 \%$
Moisture content	$\leq 8 \%$
Ash content	$\leq 1 \%$
Color	Off white

##### 3.1.2 Acid anhydride (AA) based cross linking agents

Three different types of AA cross linking agents; 1,2,4,5- benzene-tetra carboxylic anhydride (BT); 3,3'4,4'-biphenyltetracarboxylic dianhydride (DPA) and 4,4'-oxydiphtalic anhydride (ODA) with their general properties are listed in Table 3.1.

The cross linking agents were purchased from Sigma Aldrich (Malaysia) and dried at 120 °C prior to use.

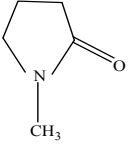
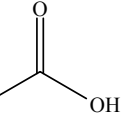
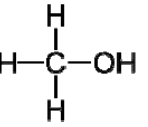
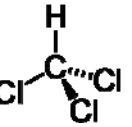
**Table 3.2:**The general properties of BT, DPA and ODA.

Properties	AA cross linking agents		
	BT	DPA	ODA
Molecular formula	 C <sub>10</sub> H <sub>2</sub> O <sub>6</sub>	 C <sub>16</sub> H <sub>6</sub> O <sub>6</sub>	 C <sub>16</sub> H <sub>6</sub> O <sub>7</sub>
Molar mass (g mol <sup>-1</sup> )	218.12	294.22	310.21
Melting point (°C)	283 to 286	299 to 305	225 to 229
Purity (%)	97	97	97
Appearance	White to light beige powder	Tan powdery; Odorless	Slightly tan ; Odorless crystalline

### 3.1.3 Organic solvents

For synthesise of XCs filler as well as the fabrication of Cs/XCs bio-composites, four types of organic solvents have been used; N-methyl pyrrolidone (NMP), acetic acid (AcOH), methanol and chloroform. The general properties of the respective organic solvents are listed in Table 3.3. All the solvent were purchased from Merck & Co (Germany).

**Table 3.3:**The general properties of NMP, AcOH, methanol and chloroform

Properties	Organic solvents			
	NMP	AcOH	Methanol	Chloroform
Molecular formula	 C <sub>5</sub> H <sub>9</sub> NO	 C <sub>2</sub> H <sub>4</sub> O <sub>2</sub>	 CH <sub>4</sub> O	 CHCl <sub>3</sub>
Molar mass (g mol <sup>-1</sup> )	99.13	60.05	32.04	119.38
Density (g cm <sup>-3</sup> )	1.028	1.049	0.79	1.48
Melting point (°C)	-24	16.5	-98	-63.5
Boiling point (°C)	202	118.1	65	61.2
Flash point (°C)	91	43	11	Non-flammable

### 3.1.4 Solid chemicals

The solid chemical used to synthesize the XCs filler were sodium hydroxide (NaOH) and phosphorous pentoxide ( $P_4O_{10}$ ). The general properties of the respective chemicals are listed in Table 3.4. Both chemicals were purchased from Sigma Aldrich (M) Sdn Bhd.

**Table 3.4:** The general properties of NaOH and PO

Properties	Solid chemicals	
	NaOH	$P_4O_{10}$
Molecular formula	NaOH	$P_4O_{10}$
Molar mass ( $gmol^{-1}$ )	39.99	283.89
Density ( $gcm^{-3}$ )	2.13	2.39
Melting point ( $^{\circ}C$ )	318	340
Boiling point ( $^{\circ}C$ )	1388	360
Appearance	White solid, hygroscopic	White powder, very pungent odor

### 3.1.5 pH buffer solutions

The pH buffer solutions were used for swelling medium and purchased from Sigma Aldrich (M) Sdn Bhd. The properties of the buffer solutions are listed in Table 3.5.

**Table 3.5:** The composition of buffer solution as corresponds to different pH

pH of buffer solution	Composition
pH 2	Citric acid, hydrochloric acid and sodium chloride
pH 4	Citric acid, hydrochloric acid and sodium chloride
pH 6	Citric acid, sodium hydroxide
pH 8	Borax, hydrochloride acid
pH 10	Borax, sodium hydroxide
pH 12	di-sodium hydrogen phosphate/sodium hydroxide solution

## **3.2 Methodology**

### **3.2.1 Purification of raw materials**

#### **3.2.1.1 Purification of Cs powder**

Cs powder (5.0 g) was mechanically mixed in AcOH (200 ml; 0.05 M) using the magnetic stirrer (50 rpm; 12 hours; 25 °C). The mixture was then filtered through wet and flat filter membrane (mesh size: 0.45 µm). The filtration process was done under the partial vacuum condition (Figure 3.1a). In order to maintain the vacuum condition, the filtration process was arranged as follows. Buchner flask, attached to the source of vacuum was used as the receiving flask. The water rushing through the water aspirator dragged the air and generated source of suction; acted as the vacuum introducer for the filtration process. To safeguard, an empty glass washing bottle (as water trap) was included between the water aspirator and the filtration apparatus. The mixture was poured and filtered onto the centre of filter membrane. The rate of water flow was systematically increased to introduce more vacuums for Buchner flask. After the filtration process was completed, the vacuum was released as the AcOH solvent was totally sucked and left the filtered products on top of filter membrane.

NaOH (1 M) was added to the filtered products for precipitation of Cs powder. As NaOH solution was in bore fluid, only a small quantity was required for the quick neutralization of the AcOH solution. The precipitated Cs powders were collected through the second filtration process and washed with plenty of distilled water until pH 7 was recorded. The pH values were recorded by the calibrated pH meter [Fisherbrand: Model AR 10].

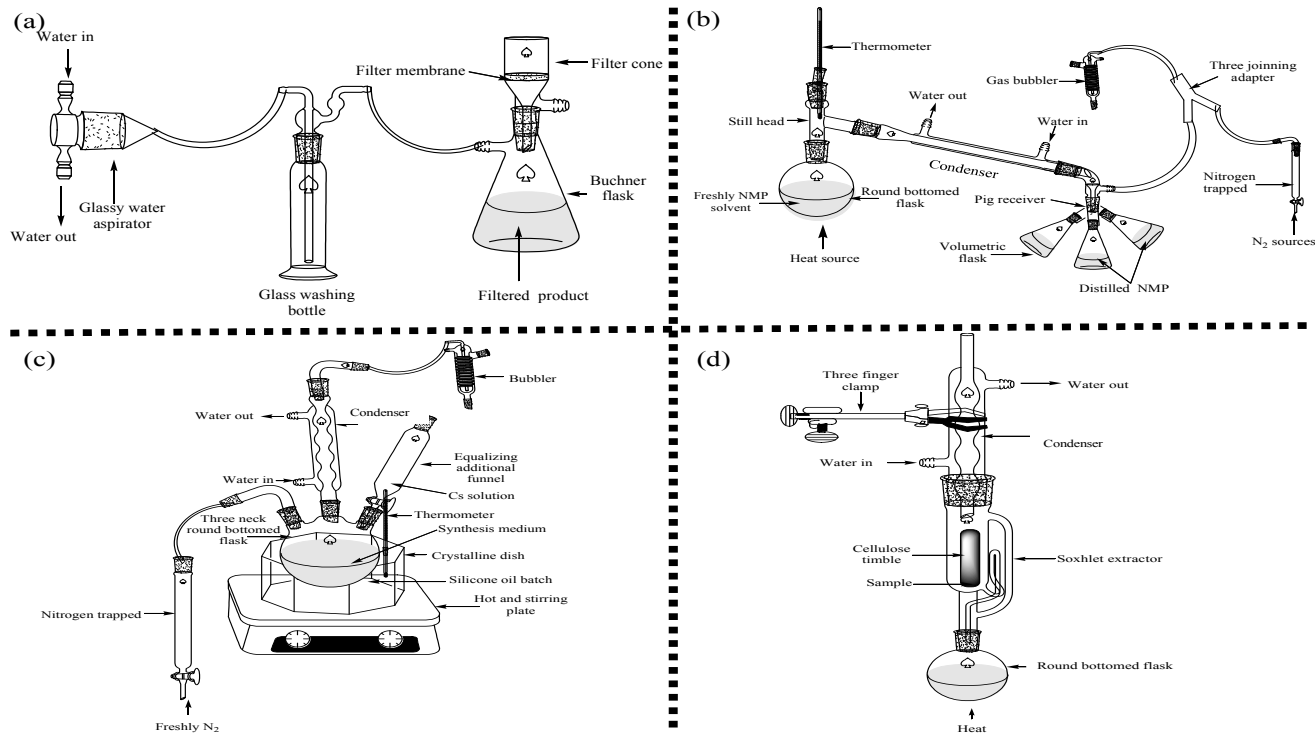


**Figure 3.1:** The glassware set up of (a) purification of raw materials (b) purification of organic solvents (c) synthesis of XCs and (d) purification of XCs

The calibration work of pH meter was done by using buffer solution pH 4 (for the acidic reference), pH 7 (for the neutral reference) and pH 10 (for the basic reference). After several washing with acetone, the neutralized Cs powders were dried overnight in a vacuum oven at 60 °C. The dried Cs powders were kept under reduced pressure in the desiccators prior to usage.

### **3.2.1.2 Distillation of NMP solvent**

The apparatus used for the distillation consists of three major parts: distillation flask (250 ml; round bottomed; single neck) to heat the NMP solvent, a condenser to cool the vapors back to liquid state and the three joint collection vessels (50 ml; flat bottomed conical flask; single neck) (Figure 3.1b). Connection between the glass parts involved rubber or cork stopper. Heating mantle (Fisher Scientific; 250 ml; 150 watts) was used as the heating sources to conform to the round bottomed flask. The adjustable jack laboratory (110X100) mm was placed as the base for the heating mantle. The round bottomed flask was filled with NMP solvent ( $\approx$  100ml). The thermometer adapter and the thermometer were fitted at such height; measures the temperature of NMP vapor not the solvent. To prevent a sudden boil, 5 to 10 of anti bumping granules were added to the freshly NMP solvent.

The condenser must be connected to a source of running water to provide enough cooling process of NMP vapors. Therefore, the input hose was connected to the condenser at the end furthest from heated flask. This prevents the hottest vapors from contacting the coldest water and creating a large thermal shock to the glass wares. The hoses must be connected tight enough to the condenser that it would not come loose if the water pressure increases during the distillation process. Therefore, copper wire was twisted around the tubing joint to prevent it from coming away. The



flow of water must be sufficient to accomplish condensation without being so fast as to cause undue hose pressure or splashing of outflow water.

The pig receiver was used as the collection vessels, to allow fractions to be isolated from the rest of the still, without the main body of the distillation being removed from the heat sources. Consequently, this could retain the distillation process in a reflux state. The reflux state can also be achieved by the introduction of inert gas. In this study, the dried  $N_2$  at the constant flow rate (1 atm) was used as inert gas. The drying process of  $N_2$  gas was done through the  $N_2$  trap. The trap was opted in a glassy column. The column was simply long, wide bore glass tubing, tapered at one end and closed with a length of flexible tubing with a screw clip. A small wad of glass wool was pushed firmly by using glass rod to the tempered end of the column. The glass wool must not tightly fit; otherwise  $N_2$  was unable to flow through the column.  $P_2O_5$  powder ( $\approx 1$  g) was then located on top of the glass wool. This was repeated until  $\frac{3}{4}$  of the column height was filled with the alternate layer of glass wool and  $P_2O_5$ . It is important to ensure that no air enters the alternate layer; to provide the decomposition of  $P_2O_5$ . Meanwhile, preparation of the trap must be handled in the hood and wearing face mask and gloves is crucial to avoid inhalation. The  $N_2$  flow was controlled by the pressure regulator. The gas bubbler filled with  $\frac{1}{4}$  of silicone oil was used as the monitor of the gas flow.

The distillation process involved 2 steps of heating process. First, the NMP solvent was heated up to  $100$  °C to remove the water content and other volatile materials. The out coming drops of liquid were collected into the first volumetric flasks, whilst the temperature at the still head went up. Second, as the heating temperature went up to  $220$  °C; the vapor pressure of NMP solvent reached the

external pressure and consequently, the NMP solvent started to boil. The heat was then kept at the constant temperature (220 °C) to maintain NMP vaporization while prohibiting other undesirable elements from vaporizing. Once the NMP had vaporized, the vapor was led into the condenser and upon cooling the NMP vapor was reverted to liquid form and was run into the receiving containers. The distillation process yielded almost 95 to 98 % of distilled NMP solvent whereby there was a slight residual content of solvent in the still bottom flask.

Generally, extra care was needed during the distillation process. First, care must be taken not to let any vapors near the control switches that may spark upon switched off and on. Second, the distillation process must be done inside a hood since the NMP solvent is flammable. Third, all the components of the distillation apparatus should be secured to a stable stand or rack to prevent it from falling over during the process. Lastly, the round bottom flask should be checked for cracks before further usage.

### **3.2.2 Preparation of XCs filler**

#### **3.2.2.1 Synthesis of XCs filler**

The apparatus used for the synthesis of XCs filler consist of a synthesis flask (250 ml; round bottomed; three necks) that joint to N<sub>2</sub> flow, a set of the condenser and equalizing additional funnel (100 ml) (Figure 3.1c) . The N<sub>2</sub> gas was first dried by flowing through the N<sub>2</sub> trapped and was connected to the first neck of the synthesis flask. The condenser was placed directly on the second neck of the synthesis flask. The top of the condenser was connected by the rubbery hoses to the gas bubbler. The pressure equalizing funnel was placed on the third neck of the

synthesis flask. It is important that each of the glass ware joints were sealed by silicone-based grease to prevent the escape of solvent vapor. A small amount of the grease was wiped onto the outer edges of the glass wares' key. The magnetic stirrer equipped with hotplate was placed as the base of the synthesis flask. The synthesis flask was  $\frac{3}{4}$  dipped into the silicon oil bath with the flat bottomed crystalline dish as the container. The thermometer bulb was completely immersed until  $\frac{1}{2}$  of the silicone oil batch to determine the temperature of reaction. Such of arrangement permit an efficient and uniform heating process. Cross linking agents (BT = 1.575 g; ODA = 2.239 g; DPA= 2.124 g) was dissolved in freshly distilled NMP solution (50 ml) in the round bottom flask (250 ml; round bottomed) under  $N_2$  flow.

Cs powder (2 g) in AcOH solution (0.1 M; 100 ml) was dropped into the solution of cross linking agent through the pressure equalizing additional funnel (1 hour; 20 rpm; 200 °C). The flowing rate of Cs solution was simply controlled by the stopcock of the pressure equalizing additional funnel. The reaction continued for another 4 hours until a clear solution was obtained. The rapid agitation produced by higher rotation of the magnetic bar to ensure the well and homogenous mixing process. The clear solution was then dissolved in distilled water at the ratio of 1:20 (ml). During the dissolving process, white precipitations were deposited and settled at the bottom of the flask. The sediments were then filtrated in accordance to Section 2.2.1.1. The filtering residue was collected and dried in the vacuum oven (24 hours; 35 °C). The dried XCs filler was then manually ground by agate mortar.

### **3.2.2.2 Purification of XCs filler**

The purification of XCs filler was done under the soxhlet extraction process (Figure 3.1d). First, the XCs filler was located into a cellulose thimble and placed in

the soxhlet extractor. The extractor was then placed on the top of a well-supported round bottomed flask (250 ml) containing of methanol ( $\text{CH}_2\text{OH}$ ) (100 ml). The reflux condenser was placed on top of the soxhlet extractor. This set up was hold and supported by three-finger clamp and support stand. The flask was heated up to  $60\text{ }^\circ\text{C}$  to ensure the boiling of  $\text{CH}_2\text{OH}$ . As the heating temperature reached to  $60\text{ }^\circ\text{C}$ , the  $\text{CH}_2\text{OH}$  vapor passed up the large diameter outer tube of the extraction apparatus. The condensed  $\text{CH}_2\text{OH}$  dropped down through the cellulose thimble. The impurities of XCs filler were extracted into the hot  $\text{CH}_2\text{OH}$ . As the condensed  $\text{CH}_2\text{OH}$  reached the top of the siphon tube, the solvent automatically passed through the narrow tube and returned to the flask; the extracted XCs filler was accumulated. The cycle was repeated for five times until the color of  $\text{CH}_2\text{OH}$  changed from colorless to yellowish. The residual of NMP solvent was removed through the extraction process. Consequently, the XCs filler was taken out from the cellulose thimble and placed onto the glassy dish. The XCs filler was dried at  $25\text{ }^\circ\text{C}$  for 6 hours to remove the remaining  $\text{CH}_2\text{OH}$ .

### **3.2.3. Preparation of Cs/XCs bio-composites**

The bio-composites mixture (100ml) was prepared as follows. First, XCs filler (2 to 14 wt/v%) mixed in AcOH solvent (95ml; 0.1 M). The mixing process was done using a magnetic stirrer (20 rpm; 2 hours;  $35\text{ }^\circ\text{C}$ ) until visually homogenous (no floating of XCs filler) mixture was observed. Then, Cs powder (2.0 g) was added and mixed continuously (50 rpm; 12 hours;  $35\text{ }^\circ\text{C}$ ). Consequently, distilled water ( $\approx 5\text{ ml}$ ) was added slowly during the mixing process to obtain 100 ml of the mixture. The mixture was heated at  $40\text{ }^\circ\text{C}$  and then vigorously mixed for 10 minutes to improve the dissolving of Cs powder. The polyethylene plate with an

enclosed framing area of (100X100X1) mm were leveled and cleaned. The mixture was cast in a circular area in the central part of the plates and then spread uniformly. The mixture was dried for approximately 48 h at 35 °C; results the Cs/XCs bio-composites. Each of the bio-composites was soaked (30 min; 35 °C) in CH<sub>2</sub>OH containing a concentrated NH<sub>4</sub>OH (0.6 wt%) solution to neutralize the remaining AcOH solvent.

### **3.2.4 Characterization of Cs, XCs and Cs/XCs bio-composites**

#### **3.2.4.1 Chemical properties**

##### **3.2.4.1a Fourier Transform Infra-red (FTIR) analysis**

The chemical structure of Cs, XCs and Cs/XCs bio-composites was identified by Fourier Transformed Infra-Red [FTIR-Model Spectrum Ones (Perkin-Elmer)] instrument. The sample was dried overnight at 60 °C under reduced pressure. The dried sample (2 mg) was mixed with the dried pure spectroscopy grade of potassium bromide (KBr) (300 to 400 mg). The mixture was ground with an agate mortar and pestle. The mixture was placed in the die of the press and was subjected to high pressure approximately of 10 tons in<sup>-2</sup> ( $\approx 1.575 \times 10^5 \text{ kgm}^{-2}$ ). The pressuring process was done by using a hydraulic press. This resulted in the formation of a very thin and fragile translucent disk with the diameter of 10 mm. The press was removed from the die with tweezers and placed in the sample beam of IR spectrometer. The resolution was 4 cm<sup>-1</sup> and there were 10 times of IR scanning applied for each spectrum. Besides the chemical structure, the degree of deacetylation (DD) of sample was calculated through FTIR analysis. The value was calculated as follows (Equation 3.1) (Brugnerotto *et al.*, 2001):

$$DD = 100 \times \frac{\left(1 - \frac{A_{1655}}{A_{3450}}\right)}{1.33}$$

Equation 3.1

where:

DD: Degree of deacetylation

A<sub>1655</sub>: Transmitted intensity at 1655 cm<sup>-1</sup>

A<sub>3450</sub>: Transmitted intensity at 3450 cm<sup>-1</sup>

### 3.2.4.1b <sup>1</sup>H and <sup>12</sup>C Nuclear Magnetic Resonance (<sup>1</sup>H <sup>12</sup>C NMR) analysis

The nuclear magnetic resonance analysis of Cs and XCs was done under the magic angle spinning on NMR [Solid State NMR; Bruker AV400] spectrometer, at a frequency of 100 612 MHz for <sup>12</sup>C NMR and 400 129 MHz for <sup>1</sup>H NMR analysis. The analysis of <sup>12</sup>C NMR was done with pulse programmed of CPMAS (cross polarization magic angle spinning), spin rate of 7 kHz, number of scan of 15 to 16 K, and recycle delay of 5sec, contact pulse of 2000 μ sec with standard reference of TMS. Meanwhile, the <sup>1</sup>H NMR analysis was done with pulse programmed of Zg30, spin rate of 7 kHz, number of scan of 5000, and recycle delay of 1 sec, contact pulse of 3 μ sec and standard reference of TMS. First the samples were ground into the fine powder and packed into a cylinder. The empty rotor was placed into the sample cylinder with its open end at the upside. The funnel of NMR machine was then placed over the rotor followed by located the piston in the funnel. The combination was shaken by hand to apply some pressure to the sample. This procedure should be repeated until the rotor was full and leave a sufficient space for fitting of the cap. It was essential that the cap was pushed all the way in and no space was left between the rotor top and collar of the cap. Lastly, the rotor was left to spin at a relatively low speed (800 to 1500) Hz for a couple of minutes before accelerated to the desired speed.

### 3.2.4.1c Elemental analysis

The elemental compositions of Cs and XCs (C, H, and N) were determined using Elemental analyzer [Perkin Elmer PE 2400 CHN and CHNS]. The DD values of samples can be derived from the elemental analysis through the following equation (Wang *et al.*, 2005):

$$DD = \frac{6.864 - \frac{C}{N}}{6.864 - 3.143} \times 100 \quad \text{Equation 3.2}$$

where:

DD: Degree of deacetylation  
C: Composition of C element (%)  
N: Composition of N element (%)

### 3.2.4.1d Energy Dispersive X-ray Spectroscopy (EDXS) analysis

The EDXS analysis of Cs and XCs was carried out with a EDXS [JEOL JPS-9200] spectrometer equipped with a monochromatic Al K $\alpha$  ( $h\nu = 1486.6$  eV) X-ray source of 12 kV X 25 mA (300 W). Pass energy for high resolution spectra of 100 eV. The area analyzed was (3 X 1) mm. A survey spectrum from 1 to 1200 eV was recorded for each sample.

### 3.2.4.2 Physical properties

#### 3.2.4.2a X-ray Diffraction (XRD) analysis

X-ray diffraction patterns of the samples were obtained by using an X-ray diffractometer [XRD: Bruker AXS D 8 Advance]. Ni-filtered Cu K $\alpha$  radiation generated at 30 kV and 30 mA with the wave number of 0.154 nm was used as the X-ray source. The sample was obtained after concentrated by a rotary evaporator, and then dried at 60 °C for 24 hours in the vacuum before being analyzed. The